

# Modulation Detection for Communication Systems

S. Selvakumar

Assistant Professor, ECE Department  
SCSVMV

M. Vinoth

Assistant Professor, ECE Department  
SCSVMV University,

G. Sathishkumar

Research scholar, ECE Department  
SCSVMV University,

**Abstract**—Receiver can be used to detect modulation formats with QPSK, DPSK, 16QAM, 32QAM, 64QAM and 256QAM. To be able to identify clear performance tendencies for high-order modulation compared with formats are investigated formats by conducting comprehensive calculations in a uniform simulation atmosphere. The influence of different transmitter structures and decision schemes is measured and all systems are characterized with respect to the signal- to-noise ratio necessities, dispersal acceptance, and self-phase- modulation performance for non-return-to-zero (NRZ) and RZ pulse shapes. Moreover, an inherent problem of QAM transmission concerning SPM is presented, and advantage techniques are observed. The results give a significant insight into the properties of high-order modulation formats. The selection of modulation scheme depends on Bit Error Rate (BER), Signal to Noise Ratio (SNR), Available Bandwidth. The basic criteria for best modulation technique are Power efficiency, better Quality of Service, cost effectiveness, bandwidth efficiency and system complexity.

**Index Terms**—Adaptive Modulation, Bit Error Rate (BER), Multilevel systems, Quadrature amplitude modulation (QAM), Signal to Noise Ratio (SNR)

## I. INTRODUCTION

Bandwidth-intensive applications will increase the traffic volume and enhance the requirements of transmission with respect to bit rate, spectral efficiency, and robustness in future core and access networks. In recent years, systems with intensity modulation and detection were optimized to achieve higher transmission robustness and lower cost. In particular, for long transmission, the transmission distances were increased by applying dispersion compensation. The interest in differential phase-shift-keying (DPSK) formats emerged with the introduction of higher data rates, particularly for 40-Gb/s systems, in order to be able to deploy higher bit rates with existing 10-Gb/s equipment. Binary phase-modulation formats (DBPSK) were shown to feature higher robustness against nonlinear effects [1]. Multilevel phase-modulation formats as differential quadrature phase-shift keying (DQPSK) [2] and 8-ary DPSK (8DPSK) [3], [4] were investigated in order to enhance spectral efficiency as well as chromatic dispersion and PMD tolerance [5]. quadrature amplitude modulation with differentially encoded phases (QAM), such as ASK-DQPSK [6] and 16-ary amplitude phase-shift keying with four amplitude and four phase states (16-APSK), which can also be denoted as 4ASK-DQPSK [7], exhibits a reduced amount of phase states for the same number of symbols.

In all the referenced systems, signals are detected by interferometry receivers, which transform the differentially encoded phase modulation into IM before photodiode square-law detection so that the critical need for frequency, phase, and polarization synchronization between the modulation signal and a local laser is avoided. On the other hand, advantages in component technology and presently available high-speed digital signal processing lay new foundations for the implementation of coherent receivers. Recently, homodyne receivers with digital phase estimation were investigated for M-ary PSK formats [8] as well as for 16-ary QAM [9]. A heterodyne detection experiment was shown even for 128QAM at 20 MBd [10].

This paper is restricted to systems and presents the performance of two 16-ary modulations formats (16DPSK and 16QAM/ASK-8DPSK) for the first time. In order to evaluate the performance tendencies of high-order modulation, the formats are compared to the already investigated formats (ASK, DBPSK, DQPSK, and 8DPSK). The intention of this comprehensive analysis is to carry out a fair comparison at 40 Gb/s, in which all the results are produced in a uniform simulation environment and using the same global parameters.

Different structures with different transmission characteristics are observed, and detailed information is included, like the implementation of the differential encoder for 16DPSK, the general theory of two equivalent receiver concepts is provided. One option is to use two delay line interferometers (DLIs) for phase detection. Another option is to employ a  $2 \times 490^\circ$  hybrid combined with a delay of one-symbol period in front of one of the hybrid inputs. It is shown that arbitrary DPSK and QAM signals with differentially encoded phases can be received. Next section describes the data-recovery process, taking into account the different decision methods. The remaining sections address the transmission properties of all the investigated modulation formats and structures for non-return-to-zero (NRZ) and return-to-zero (RZ) pulse shapes. In next section, the signal-to-noise ratio (SNR) requirements are designated by Monte Carlo (MC) simulations, and the dispersion and self-phase-modulation (SPM) tolerances are characterized by the eye-opening penalty (EOP). One main result is the poor SPM tolerance of QAM formats, which can necessitate a compensator for SPM-tolerance enhancement. Two simple compensation schemes as well as their performance gains are

illustrated this Section. A practical discussion about the properties of the modulation formats in terms of complexity and transmission characteristics is carried out.

## II. TRANSMITTERS FOR HIGH-ORDER MODULATION

In this section, the transmitter architectures are illustrated. Fig. 1 shows an overview about the constellation diagrams of the modulation formats observed in this paper. For ASK, just the intensity of the continuous-wave (CW) light is modulated, for instance, by using a Mach-Zehnder modulator (MZM). Only the binary ASK (2ASK), which can also be denoted as ON-OFF Keying (OOK), is included in the performed investigation here. RZ pulse carving can be achieved by using an additional MZM. By driving this modulator at the quadrature point with a sinusoidal signal with a frequency corresponding to the symbol rate, RZ pulses with 50% duty cycle can be generated.

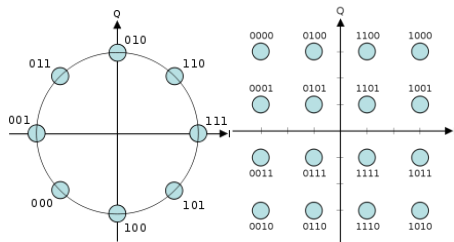


Fig. 1 Constellation diagram for DPSK and QAM

### A. DPSK Transmitters:

Generally, DPSK signals can be constituted by many different transmitter types. complexity can be reduced by increasing electrical complexity and vice versa. Moreover, the suitability of a transmitter structure depends on the particular modulation format.

From principle, in the part, a single phase modulator (PM) or MZM would be sufficient for the generation of arbitrary DPSK signals. However, for high-order DPSK, multilevel driving signals would be required. Their generation increases the electrical effort. Furthermore, system performance is degraded due to higher eye spreading when overlapping binary electrical signals to multilevel signals [11]. Another option is to use the so-called IQ-modulator, where the light is split by a 3-dB coupler into two arms, which are the in phase (I) arm and the quadrature (Q) arm.

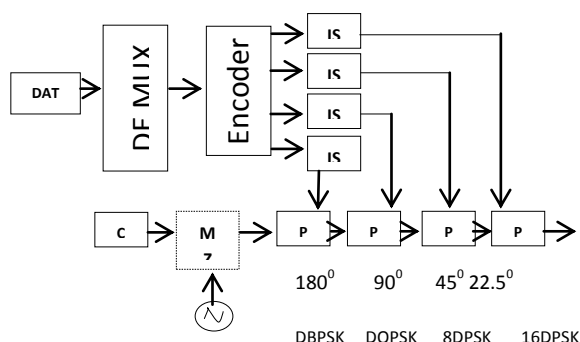


Fig. 2DPSK transmitter configurations

In the Q-arm, the light is additionally phase-shifted by  $-90^\circ$ . In every arm, an amplitude modulation is performed by an MZM, which is driven at the minimum transmission point. After that, light is recombined by a second 3-dB coupler. For a pure IQ-modulator, the necessary number of states of the electrical driving signals corresponds to the number of projections of the symbol points to the I- and Q-axes. Thus, from a practical point of view, the IQ-modulator is not the best choice for the generation of high-order DPSK signals, because all constellation points lay on one circle, and the distances between the signal states of the in phase and quadrature driving signals are small.

Our investigations are restricted to transmitters which require only binary electrical driving signals. One possibility is to use consecutive PMs, where is the number of bits per symbol. This transmitter is shown on the top part of Fig. 2 and will be called “serial transmitter” in the following. After the first PM ( $180^\circ$  phase shift), a DBPSK signal is obtained; after the second PM ( $90^\circ$  phase shift), a DQPSK signal is obtained, and so on. A second option is a combination of an IQ-modulator and consecutive PM, which is called in the following as “parallel transmitter” and shown on the bottom part of Fig. 2. The IQ-modulator accomplishes a DQPSK modulation, and high-order DPSK formats can be generated by the consecutive PM.

In the electrical part of the transmitters, the data signal first is parallelized with a 1: m DE multiplexer. Parallelized data are then fed into a differential DPSK encoder, whose configuration and complexity depend on the order of the DPSK modulation (number of phase states), the built-up of the - transmitter part, as well as the used bit mapping of the data to the constellation points. For the best OSNR performance, bit mapping should be arranged as gray coded, so that only 1 bit per symbol differs to a neighboring symbol. The bit assignment at the output of the encoders has to be chosen according to the particular transmitter configuration in order to drive the modulators adequately to obtain the appropriate absolute phase states. The functionality of the 16DPSK encoder for the serial configuration is explained. The differentially encoded binary output signals can additionally be formed by impulse shapers (IS). Afterwards, they are given to the modulators, as illustrated in Fig. 2.

The choice of the transmitter configuration will affect the transmission properties of the resulting DPSK signals, due to the fact that symbol transitions (intensity and phase transitions) of the transmitters are different, particularly for the NRZ case. As an example, the 8DPSK NRZ intensity eyes and IQ-diagrams are plotted in Fig. 3 for both investigated transmitter types. For the serial transmitter, symbol transitions are conducted on circles, and there is full intensity during phase changes. For the parallel transmitter, the power is reduced during some symbol transitions (intensity dips). This

leads to better dispersion and SPM tolerance due to reduced chirp, as shown in Section V.

### B. QAM Transmitters:

When compared to pure phase modulation, combined phase and amplitude modulation (QAM) exhibits a reduced amount of phase states for the same number of symbols. The constellation points can be arranged in a square (Square QAM formats), or they can lie on multiple circles (QAM formats). For QAM formats, the phases are arranged equally spaced, so that phase information can be differentially encoded as for DPSK formats (phase differences take the same values as the absolute-phase values). Thus, QAM signals with differentially encoded phases can be detected by receivers. Square QAM signals, however, have to be detected by coherent techniques.[12]

For generation of QAM signals with differentially encoded phases, the same equipment can be used as for the just-described DPSK transmitters. Only an additional MZM for IM has to be inserted to be able to place symbols on different circles. AQAM format, which was already investigated in [6], is 8QAM (ASK-DQPSK). An 8QAM transmitter can be composed of a DQPSK transmitter and an additional MZM. Same differential encoders as for DQPSK are appropriate.

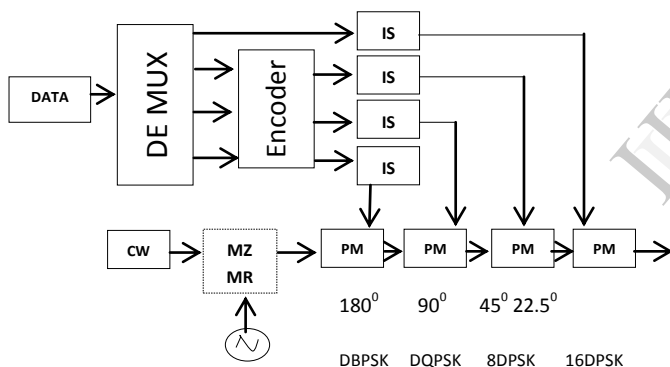


Fig 3 DPSK transmitter Serial configurations

One degree of freedom, which has to be optimized for QAM formats with respect to OSNR performance, is the ring ratio (RR)  $r_2/r_1$ , where  $r_1$  and  $r_2$  are the amplitudes of the inner and outer circles. This will be done in this section.

Principally, arbitrary QAM constellations are possible. AQAM constellation with 16 symbols, which is composed of four amplitude and four phase states, was investigated in [7]. The definition of only four phase states has the advantage of an easier data recovery within the receivers. On the other hand, the use of more than two amplitude states does not allow for RR optimization and leads to high OSNR requirements for intensity detection and, thus, to bad overall OSNR performance.

## III. RECEIVERS FOR HIGH-ORDER MODULATION

Compared to coherent receivers, receivers convince with their simplicity. No phase, frequency, or polarization control is necessary. On the other hand, only the intensity of the field can be detected. However, also the phase information of signals can be obtained when using additional optics. If the phase was differentially encoded at the transmitter, phase (difference) information can be converted to intensity information by an interferometer, which can then be detected by a photodiode. With an intensity-detection branch added to the phase-detection branch, the QAM detection can also be performed.[13]

In this section, the fundamental receiver theory is described. Two receiver structures are shown to be equivalent under certain circumstances. A first option is to convert phase modulation to IM with DLIs. The outputs of the DLIs are detected by balanced detectors (BDs). Using two DLIs with adequate phase shifts, in phase and quadrature components are obtained, and thus, every DPSK format can be detected. Furthermore, it is possible to displace the two DLIs by a  $2 \times 4$  90° hybrid and a delay of one-symbol duration in front of one of the hybrid inputs. Both receiver options are shown in Fig. 4. We start with the theoretical description of the receiver constituted by two DLIs. The incoming normalized electrical field of the multilevel modulation signal can be written in complex notation (neglecting transmission impairments) as

$$E_s(t) = a(t)\sqrt{P_s}e^{j(\omega_s t + \phi_s + \phi_{NS}(t) + \phi(t))} \quad (1)$$

In (1),  $P_s$  represents the CW power,  $\omega_s$  represents the angular frequency,  $\phi_s$  represents the initial phase, and  $\phi_{NS}(t)$  represents the phase noise of the signal laser. The normalized modulation amplitude and the differentially encoded phase information are represented by  $a(t)$  and  $\phi(t)$ , respectively. The signal is split by a 3-dB coupler and given to

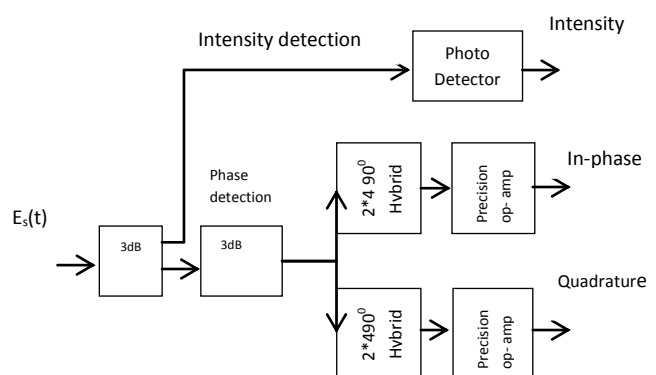


Fig 4 Higher order modulation Receiver

two branches, which are the intensity-detection branch and the phase-detection branch. The output current of the photodiode in the intensity-detection branch is,

$$I_{PD}(t) = R \frac{E_s(t)}{\sqrt{2}} \cdot \frac{E_s^*(t)}{\sqrt{2}} = \frac{1}{2} R a^2(t) P_s \quad (2)$$

Where  $R$  is the responsivity of the photodiode, and “\*” denotes conjugate complex operation. The photocurrent given by (2) is proportional to the CW power and the square of the normalized modulation amplitude. Thus, the intensity of a symbol is detected in the intensity-detection branch. The second output of the first 3-dB

$$E_I(t) = \frac{a(t)\sqrt{P_s}}{2} e^{j(\omega_s t + \varphi_s + \varphi_{NS}(t) + \varphi(t))} \cdot e^{j90^\circ} \quad (3)$$

$$E_Q(t) = \frac{a(t)\sqrt{P_s}}{2} e^{j(\omega_s t + \varphi_s + \varphi_{NS}(t) + \varphi(t))} \cdot e^{j180^\circ} \quad (4)$$

Coupler meets the phase- detection branch and is split by a second 3-dB coupler for the detection of the in phase and quadrature components. Taking into account the phase shifts of the couplers, two fields with a phase difference of  $90^\circ$  are obtained at the upper and the lower outputs of the second 3-dB coupler.

#### A. DATA RECOVERY

In this section, it will be shown how the data recovery can be accomplished for the different modulation formats, when using thereceiver with two DLIs or the receiver with  $2 \times 4$   $90^\circ$  hybrid.

$$\begin{aligned} E_{QI,1}(t) &= \frac{a(t-T_s)\sqrt{P_s}}{4} e^{j(\omega_s t + \varphi_s + \varphi_{NS}(t-T_s) + \varphi(t-T_s))} \cdot e^{j90^\circ} \\ &+ \frac{a(t)\sqrt{P_s}}{4} e^{j(\omega_s t + \varphi_s + \varphi_{NS}(t) + \varphi(t))} \cdot e^{j270^\circ} \cdot e^{j\varphi_I} \end{aligned} \quad (5)$$

$$\begin{aligned} E_{QI,2}(t) &= \frac{a(t-T_s)\sqrt{P_s}}{4} e^{j(\omega_s t + \varphi_s + \varphi_{NS}(t-T_s) + \varphi(t-T_s))} \cdot e^{j180^\circ} \\ &+ \frac{a(t)\sqrt{P_s}}{4} e^{j(\omega_s t + \varphi_s + \varphi_{NS}(t) + \varphi(t))} \cdot e^{j180^\circ} \cdot e^{j\varphi_I} \end{aligned} \quad (6)$$

After electrical low-pass filtering, the in phase and quadrature photocurrents in the phase-detection branch can be processed by different techniques to recover the data information corresponding to the phase bits. These techniques differ in the positioning of the thresholds and their practical implementation and are shown in Fig. 5

$$\varphi_{NS}(t) \approx \varphi_{NS}(t - T_s) \quad (7)$$

For maximum distances between symbols and thresholds and for best performance, the thresholds should be positioned radially between the two phase states, as shown for 8DPSK and 16DPSK on the bottom part.

$$\Delta\varphi(t) = \varphi(t) - \varphi(t - T_s) \quad (8)$$

In the following, this type of decision will be denoted as “argdecision.” By performing an arg-operation (calculation of the angle of a complex value) on the in phase and quadrature signals, a multilevel signal arises, whose states represent the received phase differences. Decision is then performed on these multilevel signals,

$$I_{I,1} = RE_{I,1} E_{I,1}^* \quad (9)$$

$$I_{I,1} = RE_{I,2} E_{I,2}^* \quad (10)$$

Applying the radially positioned thresholds, the outcome of the decision is then processed by appropriate data-recovery logic to obtain the data bits, which, finally, can be multiplexed to obtain the original data stream. In practice, the arg-operation could be implemented by digital means, and the performance will then depend on the resolution of the used analog-digital (A/D) converter. In the investigations of this paper, the A/D converter is assumed to be ideal.

$$I_I(t) = R \frac{a(t)a(t-T_s)P_s}{4} \cos[\Delta\varphi(t) + \varphi_I] \quad (11)$$

$$I_Q(t) = R \frac{a(t)a(t-T_s)P_s}{4} \cos[\Delta\varphi(t) + \varphi_Q] \quad (12)$$

Another option is to perform the decisions directly on the in phase and quadrature photocurrents, as shown in Fig. 5 (bottom).

$$I_I(t) = R \frac{a(t)a(t-T_s)P_s}{4} \cos[\Delta\varphi(t)] \quad (13)$$

$$I_Q(t) = R \frac{a(t)a(t-T_s)P_s}{4} \sin[\Delta\varphi(t)] \quad (14)$$

This technique will be denoted as “IQ-decision” in the following. For DBPSK (only the in phase branch is required) and DQPSK, the decisions are performed on binary signals at a threshold of zero. For high-order DPSK formats, in phase and quadrature signals are multilevel, and the decision modules have multiple thresholds, as shown for 8DPSK on the top right part and already described in [6].

$$E_1(t) = \frac{a(t)\sqrt{P_s}}{2} e^{j(\omega_s t + \varphi_s + \varphi_{NS}(t) + \varphi(t))} \cdot e^{j90^\circ} \cdot e^{j\varphi} \quad (15)$$

$$E_2 = \frac{a(t-T_s)\sqrt{P_s}}{2} e^{j(\omega_s t + \varphi_s + \varphi_{NS}(t-T_s) + \varphi(t-T_s))} \cdot e^{j90^\circ} \cdot e^{j\varphi} \quad (16)$$

The binary data at the output of the decision modules have to be processed by appropriate data-recovery logic, which is different from the one for arg-decision. For IQ-decision, the thresholds are not optimally placed between the symbol points, so a worse OSNR performance can be expected than for ideal arg-decision.



$$\begin{bmatrix} E_{Q,2}(t) \\ E_{I,2}(t) \\ E_{Q,1}(t) \\ E_{I,1}(t) \end{bmatrix} = \frac{1}{2} \begin{bmatrix} 1 & 1 \\ 1 & j \\ 1 & -1 \\ 1 & -j \end{bmatrix} \cdot \begin{bmatrix} E_1(t) \\ E_1(t) \end{bmatrix} = \begin{bmatrix} \frac{E_1(t)}{2} + \frac{E_1(t)}{2} \\ \frac{E_1(t)}{2} + j\frac{E_1(t)}{2} \\ \frac{E_1(t)}{2} - \frac{E_1(t)}{2} \\ \frac{E_1(t)}{2} - j\frac{E_1(t)}{2} \end{bmatrix} \quad (17)$$

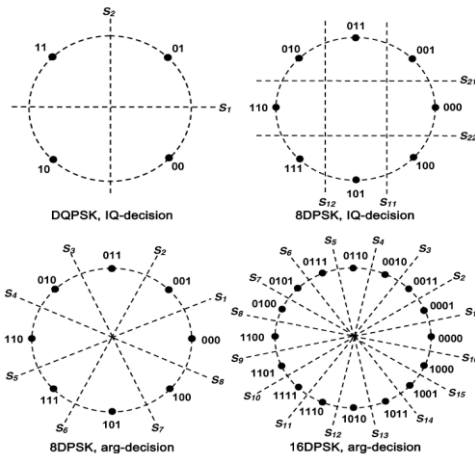


Fig 5. Used bit mapping and positioning of the thresholds for DPSK data recovery

To better understand the reconstruction of bit information for DPSK formats, the data-recovery logic is now illustrated on an example of 16DPSK. Only ideal arg-decision is considered for 16DPSK, because IQ-decision is expected to exhibit very poor performance due to the small distances between the signal levels and the thresholds in the in phase and quadrature arms. Amplitudes of two consecutive symbols, the received constellation diagrams for 8QAM (ASK-DQPSK) and 16QAM (ASK-8DPSK)

$$I_I(t) = I_{I,2}(t) - I_{I,1}(t) = R \cdot \frac{a(t) \cdot a(t-T_s) \cdot p_s}{4} \cdot \cos[\Delta\varphi(t) + \varphi] \quad (18)$$

$$I_Q(t) = I_{Q,2}(t) - I_{Q,1}(t)$$

$$= R \cdot \frac{a(t) \cdot a(t-T_s) \cdot p_s}{4} \cdot \sin[\Delta\varphi(t) + \varphi] \quad (19)$$

It can be observed that the originally two amplitude states have changed to three possible amplitude states after the process.

$$a_k = s_8 + \overline{s_{16}} \quad (20)$$

$$b = s_4 + \overline{s_{12}} \quad (21)$$

$$c_k = s_2 \overline{s_6} + s_{10} \overline{s_{14}} \quad (22)$$

$$d_k = s_1 \overline{s_3} + s_5 \overline{s_7} + s_9 \overline{s_{11}} + s_{13} \overline{s_{15}} \quad (23)$$

With the arg-decision technique, it is still possible to designate the phase-difference information. The amplitude bit is recovered by a binary decision in the intensity-detection branch, and the phase-difference information is obtained by performing the arg-operation.

$$I_I(t) = \frac{1}{2} \cdot \cos[\Delta\varphi(t)] \quad (24)$$

$$I_Q(t) = \frac{1}{2} \cdot \sin[\Delta\varphi(t)] \quad (25)$$

## B. TRANSMISSION PROPERTIES

The illustration of the transmitter and receiver configurations in the last sections gave an insight in their functionality and complexity as well as the effort which has to be undertaken for the realization of particular modulation formats. However, of at least equal importance is the knowledge of the transmission characteristics. To characterize the modulation formats with respect to their OSNR requirements, their dispersion tolerance, and their SPM tolerance, and to be able to recognize the tendencies, a wide range of modulation formats was analyzed in a comprehensive investigation. The investigation covers NRZ and RZ signals as well as the different transmitter structures and decision methods.

## C. OSNR Requirements

The OSNR requirements of all investigated systems were determined by back-to-back MC simulations for a fixed data rate of 40 Gb/s using an iterative 212 de Bruijn sequence and assuming fixed and electrical filter bandwidths of BOPT = 2.5 × symbol rate and BEL = 0.75 × symbol rate. For optimum bandwidths, OSNR requirements will relax by some tenths of decibels for particular formats. The thresholds were positioned at the middle of the signal states, except for ASK and the intensity branch for 16QAM, where the threshold was optimized. The sample time was chosen fixed at the middle of the symbols. The OSNR is defined by the signal power divided by the noise power in 0.1-nm bandwidth. Simulation results for (top) NRZ and (bottom) RZ when using the serial transmitters and arg-decision for all the modulation formats. It can be observed that RZ pulse shape performs better than NRZ for all formats, because the distances between the symbols are larger for same average power. The OSNR requirements are roughly determined by the Euclidean distances, so that modulation formats with higher spectral efficiency require a higher OSNR. When looking at the DPSK formats, DQPSK requires lower OSNR than ASK, but 8DPSK is already significantly worse. When comparing the two 16-ary modulation formats, 16QAM requires by far less OSNR than 16DPSK, and the performance is almost as good as for 8DPSK.

$$\Phi_{NL} = -\frac{2\pi n_2 f_s}{c A_{eff}} \cdot \frac{10 P_{in}(t)}{\ln 10 \cdot \alpha_{dB}} \cdot \left( 10^{-\frac{\alpha_{dB} L}{10}} - 1 \right) \quad (26)$$

The curves for 16QAM for the optimum RR (ratio between the amplitudes of the outer and inner circles). This can be observed from the top part, where the bit error rate is depicted for different RRs for a fixed OSNR (20.46 dB for NRZ and 18.46 dB for RZ) when using serial transmitters and arg-decision. Similar results were obtained for parallel transmitters and IQ-decision, where the optimal RR for NRZ was found to be 1.65 for NRZ and 1.6 for RZ, as shown on the bottom part.

$$\phi_{NL} [\text{rad}] = 27.825 \cdot p_{in}(t) [W]. \quad (27)$$

For an illustration of the influence of the transmitter structure and the decision method on the OSNR requirements, exemplarily, the comparison is shown for 8DPSK and 16QAM. However, conclusions are valid for every format. For RZ pulse shape, it makes no difference if the serial or the parallel transmitter is used, because there is almost no power during symbol transitions.

$$\begin{aligned} \phi_{NL} [\text{rad}] &= 27.825 \cdot p_{out}(t) [W] \cdot 10^{\frac{\alpha_{dB} L}{10}} \\ &= 1107.7 \cdot p_{out}(t) [W] \end{aligned} \quad (28)$$

For NRZ, however, the serial transmitters lead to worse performance due to higher chirp and, as a consequence, larger distortions at the receiver filter. When comparing the decision methods, arg-decision shows slightly better performance than IQ-decision, as it was already expected in Section IV. For arg-decision, thresholds are optimally placed between the symbols, whereas for IQ-decision, the distances between the thresholds and the symbols are slightly smaller.

#### IV. DISCUSSION

The knowledge of the transmitter and receiver structures, as well as the transmission properties of a wide range of modulation formats, now allows us to discuss their particular advantages, drawbacks, and peculiarities. In Table I, the modulation formats are compared with respect to complexity of the electrical and transmitter and receiver parts. ASK acts as reference ("0"), and all the other formats are characterized with one or more "+" to evaluate the particular complexity. The complexity of the electrical part of the transmitters depends mainly on the necessary effort for the differential encoder, because all the investigated transmitters get by with binary electrical driving signals, and no generation of multilevel driving signals is necessary. The 16DPSK transmitter needs by far the most complex differential encoder, as illustrated in the Appendix. When comparing the part of the transmitters, the effort for realization of an IQ-modulator within the parallel transmitters is higher than for realization of a pure serial configuration. Furthermore, the effort increases with the order of the modulation format and the corresponding increasing number of modulators.

The part of DPSK receivers is identical for DQPSK, 8DPSK, and 16DPSK modulation. For DBPSK, only

one branch is needed. For QAM formats, the additional intensity-detection branch increases slightly the complexity compared to DPSK receivers. The complexity of the electrical part of the receivers is determined primarily by the number of decision circuits and the built-up of the data-recovery logic. Thus, it increases by increasing the order of the modulation format. The effort for IQ-decision is almost the same as for the arg-decision for DPSK formats but higher for 16QAM, because the additional "normalization" operation, which is described in Section IV, becomes necessary.

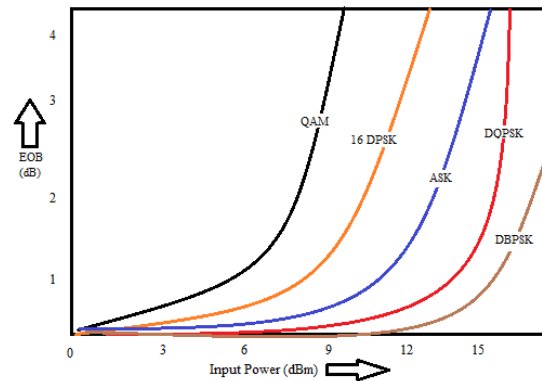


Fig. 6 Comparison result of QAM and DPSK

Generally, the complexity of the -transmitter part can be reduced by using pure IQ-modulators. On the other hand, this would increase electrical complexity, because multilevel electrical driving signals would have to be generated. Table II summarizes the transmission characteristics of all the investigated modulation formats and structures. The use of DBPSK instead of ASK leads to better OSNR performance and, first of all, to a significant enhancement of SPM tolerance for almost similar dispersion tolerance. DQPSK seems to be a very attractive candidate for future networks. The OSNR requirements are still more relaxed than for ASK and only slightly higher than for DBPSK. However, the dispersion tolerance can be enhanced by a factor of 4 for RZ pulse shape, with almost the same SPM tolerance. When migrating to higher modulation formats, the dispersion tolerance can be further enhanced, but this comes along primarily with stronger OSNR requirements. Furthermore, SPM tolerance decreases, but only slightly, for the DPSK RZ formats.[14]

From the comparison of the two 16-ary modulation formats 16DPSK and 16QAM, it can be concluded that 16QAM shows clear advantages with respect to OSNR requirements. On the other hand, SPM tolerance in the phase-detection branch is very bad due to the effect explained in Section VI. However, it can be enhanced to values almost as for 16DPSK using relatively simple SPM compensators. Generally, RZ pulse shape leads to much better system performance than NRZ with respect to all investigated criteria. An exception is the dispersion tolerance for 2ASK, binary DPSK, and DQPSK when using the parallel transmitter. In particular, the serial transmitters have poor performance for NRZ. An interesting question for further research would be

how the transmission properties presented here can be transferred into transmission reach. Whether the application of a particular modulation format makes sense or not, it will also depend on the particular network segment (core, metro, and access).

## V.CONCLUSION

Two 16-ary modulation formats, which are the DPSK and the QAM, were characterized for transmission for the first time. To evaluate the results and to be able to identify clear performance tendencies for high order modulation, their performance was opposed to a wide range of already investigated formats by conducting comprehensive calculations. Moreover, different transmitter and receiver options and different pulse shapes were covered by the investigations, and important implementation details were provided. The results of this paper allow to tradeoff different high-order modulation formats with respect to system complexity and transmission robustness. For instance, the RZ pulse shape shows advantages over NRZ in almost any case but, particularly, for high-order formats and when using transmitters with consecutive serial PMs. DQPSK is a promising candidate for future networks, with more relaxed OSNR requirements, higher dispersion tolerance, and better SPM performance than 2ASK. On the other hand, this comes along with higher transmitter and receiver complexity. When looking at even higher formats such as 8DPSK, 16DPSK, and 16QAM, dispersion tolerance can be significantly enhanced, but OSNR requirements increase, SPM tolerance decreases, and the effort for the transmitters and receivers goes up. When comparing the two 16-ary formats, 16QAM shows clear advantages over 16DPSK concerning the required OSNR, but an SPM compensator becomes necessary to enhance the poor SPM tolerance, which is caused by the unequal non-linear phase shift for symbols on different intensity rings.

## REFERENCES

- [1] M. Rohde, C. Caspar, N. Hanik, N. Heimes, M. Konitzer, and E.-J. Bachus, "Robustness of DPSK direct detection transmission format in standard fiber WDM systems," *Electronics Letter*, vol. 36, no. 17, pp. 1483–1484, 1999.
- [2] C. Wree, J. Leibrich, and W. Rosenkranz, "Differential quadrature phase-shift keying for cost-effective doubling of the capacity in existing WDM systems," *ITG-Fachtagung Photonische Netze*, Germany, 2003, pp. 161–168.
- [3] M. Ohm, "8-DPSK and receiver with direct detection and multilevel electrical signals," in *Proc. IEEE/LEOS Advance Modulation Formats*, 2004, pp. 45–46.
- [4] H. Yoon, D. Lee, and N. Park, "Performance comparison of 8-ary differential phase-shift keying systems with different electrical decision schemes," *Opt. Express*, vol. 13, no. 2, pp. 371–376, 2005.
- [5] W. Rosenkranz, "Robust multi-level phase shift modulation in high-speed WDM transmission," *Proc. SPIE*, vol. 5625, pp. 241–252, 2005.
- [6] M. Ohm and J. Speidel, "Receiver sensitivity, chromatic dispersion tolerance and optimal receiver bandwidths for 40 Gb/s 8-level ASK-DQPSK and 8-DPSK," in *Proc. 6th Conf. Photon Network*, Leipzig, Germany, May 2005, pp. 211–217.
- [7] K. Sekine, N. Kikuchi, S. Sasaki, S. Hayase, C. Hasegawa, and T. Sugawara, "Proposal and demonstration of 10-Gsymbol/sec 16-ary (40 Gb/s) modulation/demodulation scheme," in *Proc. ECOC*, 2004, pp. 424–425.
- [8] K. Kikuchi, "Coherent detection of phase-shift keying signals using digital carrier-phase estimation," presented at the *Fiber Communication (OFC)*, Anaheim, CA, 2006, Paper OTuI4.
- [9] M. Seimetz, "Performance of coherent square-16-QAM-systems based on IQ-Transmitters and homodyne receivers with digital phase estimation," presented at the *Nat. Fiber Optic Engineers Conf. (NFOEC)*, Anaheim, CA, 2006, Paper NWA4.
- [10] M. Nakazawa, M. Yoshida, K. Kasai, and J. Hongou, "20 Msymbol/s, 128 QAM coherent transmission over 500 km using heterodyne detection with frequency-stabilized laser," presented at the *(ECOC)*, Cannes, France, 2006, Paper Mo4.2.2.
- [11] K.-P. Ho and H.-W. Cui, "Generation of arbitrary quadrature signals using one dual-drive modulator," *J. Lightw. Technol.*, vol. 23, no. 2, pp. 764–770, Feb. 2005.
- [12] M. Seimetz and C.-M. Weinert, "Options, feasibility and availability of  $2 \times 490$ -hybrids for coherent systems," *J. Lightw. Technol.*, vol. 24, no. 3, pp. 1317–1322, Mar. 2006.
- [13] G. P. Agrawal, *Nonlinear Fiber Optics*. San Diego, CA: Academic, 1995.
- [14] K.-P. Ho, *Phase Modulated Optical Communication Systems*. New York: Springer-Verlag, 2005.